

Estimation of Turbulence Parameters in Pool Scrubbing Conditions

Erol Bicer^{1,2}, Shiwang Li³, Yixiang Liao*³

¹FNC Technology, Heungdeok IT Valley, Heungdeok 1-ro, Giheung-gu, Yongin-si, Gyeonggi-do, 446-908, Korea

²Seoul National University, Department of Nuclear Engineering, 1 Gwanak-ro, Gwanak-gu, Seoul 08826, Korea

³Helmholtz-Zentrum Dresden-Rossendorf, Institute of Fluid Dynamics, Bautzner Landstraße 400, 01328, Dresden, Germany

*Email: y.liao@hzdr.de

1. INTRODUCTION

1 Pool Scrubbing Process and Mechanisms

- Pool scrubbing is commonly used to retain aerosol particles
- The scrubbing process involves injection and swarm zones, each with different mechanisms
- The disintegration of large globules in the injection zone affecting the retention efficiency

2 Turbulence Modeling Challenges in Pool Scrubbing

- Turbulence is a key factor affecting bubble breakup, and thus retention efficiency
- Both shear- and bubble-induced turbulence need to be considered

3 Objectives

- Evaluate two typical turbulence models (mixtureKEpsilon and kOmegaSST) for pool scrubbing experiments
- Discuss the importance of turbulence boundary conditions for bubble column simulations
- Propose an approach for proper estimation of inlet turbulent boundary conditions

2. METHODOLOGY

Experiment and Simulation Tool

- Two pool scrubbing experiments by Abe et al. [1] and Yoshida et al. [2] are used for the investigation
- Both facilities injected air at atmospheric pressure into stagnant water and measured several parameters at various depths in a rectangular column with a 1 m submergence (see Figure 1)
- Abe et al. [1] used a single nozzle having 6 mm in diameter, while in Yoshida et al. [2] it has 10 mm in diameter
- The multiphaseEulerFoam solver in OpenFOAM V10, which is a solver for a system of many compressible fluid phases with a common pressure but otherwise separate properties, is used for the Euler-Euler simulation

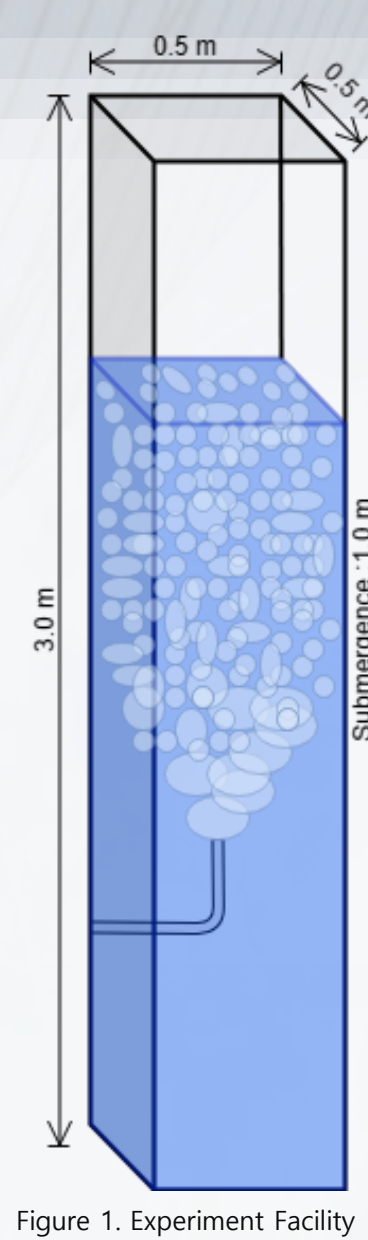


Figure 1. Experiment Facility

Typical Flow Field in Pool Scrubbing

- The instantaneous and mean void fraction and air velocity results for a diagonal cross-section of the area are presented in Fig.2 for Yoshida et al. [2] display a typical behavior of pool scrubbing column
- Results indicate that both the void fraction and gas velocity dissipate toward downstream
- Figure 3 displays the plots of the velocity vectors for both air and water. Despite the water is initially at rest, injection of air at 6.37 m/s causes the water velocity to rise up to 1.4 m/s in the proximity of the transition region
- The water velocity vector plot shows that recirculation flow, crucial for pool scrubbing in the swarm region, is generated on both sides of the column. To accurately predict recirculation flows in a large pool, a multidimensional approach is necessary through advanced turbulence and transport model

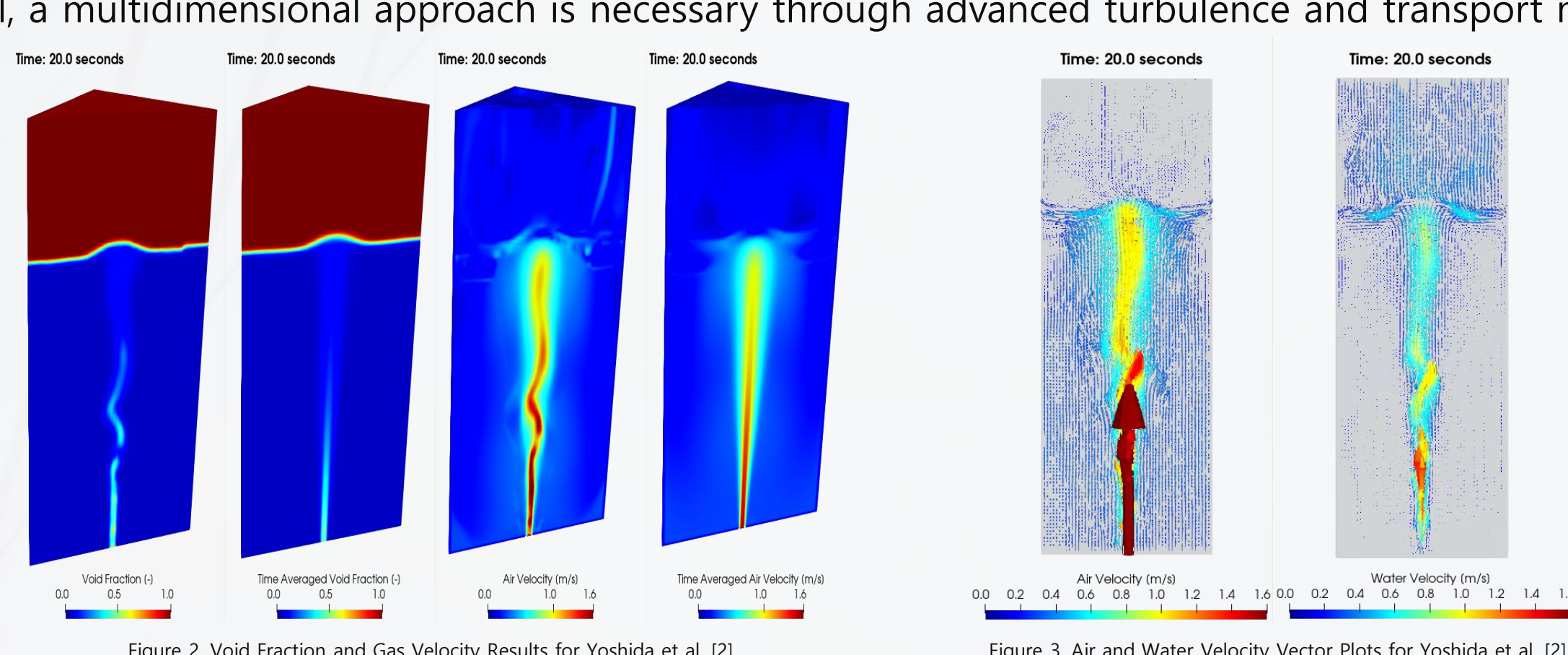


Figure 2. Void Fraction and Gas Velocity Results for Yoshida et al. [2]



Figure 3. Air and Water Velocity Vector Plots for Yoshida et al. [2]

Turbulence Modelling

- The paper compares mixtureKEpsilon [3] and kOmegaSST [4] turbulence modeling approaches, including the effect of Bubble Induced Turbulence (BIT)

1. mixtureKEpsilon model

$$\frac{\partial(\rho_m k_m)}{\partial t} + \nabla \cdot (\rho_m U_m k_m) = \nabla \left[\left(\mu_{MOL} + \frac{\mu_{m-SIT}}{\sigma_k} \right) \nabla k_m \right] + P_{k,m} - \rho_m \varepsilon_m + S_{k,m}$$

$$\frac{\partial(\rho_m \varepsilon_m)}{\partial t} + \nabla \cdot (\rho_m U_m \varepsilon_m) = \nabla \left[\left(\mu_{MOL} + \frac{\mu_{m-SIT}}{\sigma_\varepsilon} \right) \nabla \varepsilon_m \right] + \frac{\varepsilon_m}{k_m} (C_1 P_{k,m} - C_2 \rho_m \varepsilon_m) + C_3 \frac{\varepsilon_m}{k_m} S_{k,m}$$

- The velocity fluctuations induced by liquid displacement due to the relative velocity and the liquid eddies which may be formed behind the bubbles is added in the source term $S_{k,m}$ [5]

$$S_{k,m} = \frac{k_{cl}}{C_e \varepsilon_{cl}} S_e = C_p \left(1 + C_D^{4/3} \right) \alpha_g \frac{|U_r|^3}{D_b}$$

2. kOmegaSST model

$$\frac{\partial(\alpha_L \rho_L k_L)}{\partial t} + \nabla \cdot (\alpha_L \rho_L U_L k_L) = \nabla \cdot \left(\alpha_L \left(\mu_L^{mol} + \frac{\mu_L^{turb}}{\sigma_k} \right) \nabla k_L \right) + \alpha_L (P_k - \rho_L C_{\omega} k_L \omega_L) + S_L^k$$

$$\frac{\partial(\alpha_L \rho_L \omega_L)}{\partial t} + \nabla \cdot (\alpha_L \rho_L U_L \omega_L) = \nabla \cdot \left(\alpha_L \left(\mu_L^{mol} + \frac{\mu_L^{turb}}{\sigma_\omega} \right) \nabla \omega_L \right) + \alpha_L \left(C_{\omega p} \frac{\rho_L}{\mu_L^{turb}} P_k - C_{\omega D} \rho_L \omega_L^2 \right) + (1 - F_1) 2 \alpha_L \rho_L \frac{\nabla k_L \nabla \omega_L}{\sigma_\omega \omega_L} + S_L^\omega$$

- The BIT source terms, S_L^k and S_L^ω calculated according to a model derived from DNS of bubble column [6]

$$S_L^k = \min(0.18 Re^{0.23}, 1.0) \frac{3 \rho_L \alpha_L C_D}{4 d_b} |\mathbf{u}_G - \mathbf{u}_L|^3 \quad S_L^\omega = 0.3 C_D \frac{S_L^k}{\tau}, \text{ with } \tau = \frac{d_b}{|\mathbf{u}_G - \mathbf{u}_L|}$$

- The source term in the ω -equation is derived from the relation between k , ε and ω

$$S_L^\omega = \frac{1}{C_\mu k_L} S_L^k - \frac{\omega_L}{k_L} S_L^k$$

References

- [1] Abe, Y., Fujiwara, K., Saito, S., Yuasa, T., & Kaneko, A. Nuclear Engineering and Design, 337, 96-107, (2018).
 [2] Yoshida, K., Fujiwara, K., Nakamura, Y., Kaneko, A., & Abe, Y. Nuclear Engineering and Design, 388, 111645, (2022).
 [3] Behzadi, A., Issa, R. I., & Rusche, H. Chemical Engineering Science, 59(4), 759-770, (2004).

3. BOUNDARY CONDITIONS

Inlet Turbulent Boundary Conditions

- Despite its importance, there is no direct method to estimate the inlet turbulent boundary conditions for bubble column
- The Standard Pipe Flow Approach (PFA) based on mixing length scale and turbulent intensity for fully-developed pipe flow is widely used (see the right-hand side)
- For the three cases ($\dot{Q} = 30, 60, 90$ lpm) from Yoshida et al. experiment, PFA provides following inlet conditions

Case	L _c [m]	Re [-]	L _m [m]	CT _i [-]	CT _i [%]	k _{in} [m ² /s ²]	ε _{in} [m ² /s ³]	v _i [m ² /s]	v _{mol} [m ² /s]
#1	0.01	4215.36	0.0007	0.0564	5.64%	1.934E-01	1.996E+01	1.686E-04	
#2	0.01	8424.11	0.0007	0.0517	5.17%	6.495E-01	1.229E+02	3.090E-04	1.511E-05
#3	0.01	12639.47	0.0007	0.0491	4.91%	1.321E+00	3.564E+02	4.407E-04	

1. Calculate the Reynolds Number:

$$Re = \frac{\rho U L_c}{\mu} \equiv \frac{U L_c}{v}$$

2. Calculate the Turbulent Intensity:

$$T_i = 0.16 Re^{-1/8}$$

3. Calculate the Turbulent Kinetic Energy:

$$k_{in} = \frac{3}{2} (UT_i)^2$$

4. Calculate the Inlet Energy Dissipation:

$$\varepsilon_{in} = C_\mu \frac{k_{in}^{3/2}}{L_m}$$

5. Calculate the Eddy Viscosity:

$$\nu_t = C_\mu \frac{k_{in}^2}{\varepsilon_{in}}$$

L_c , L_m is the characteristic and mixing length scale, respectively

4. RESULTS

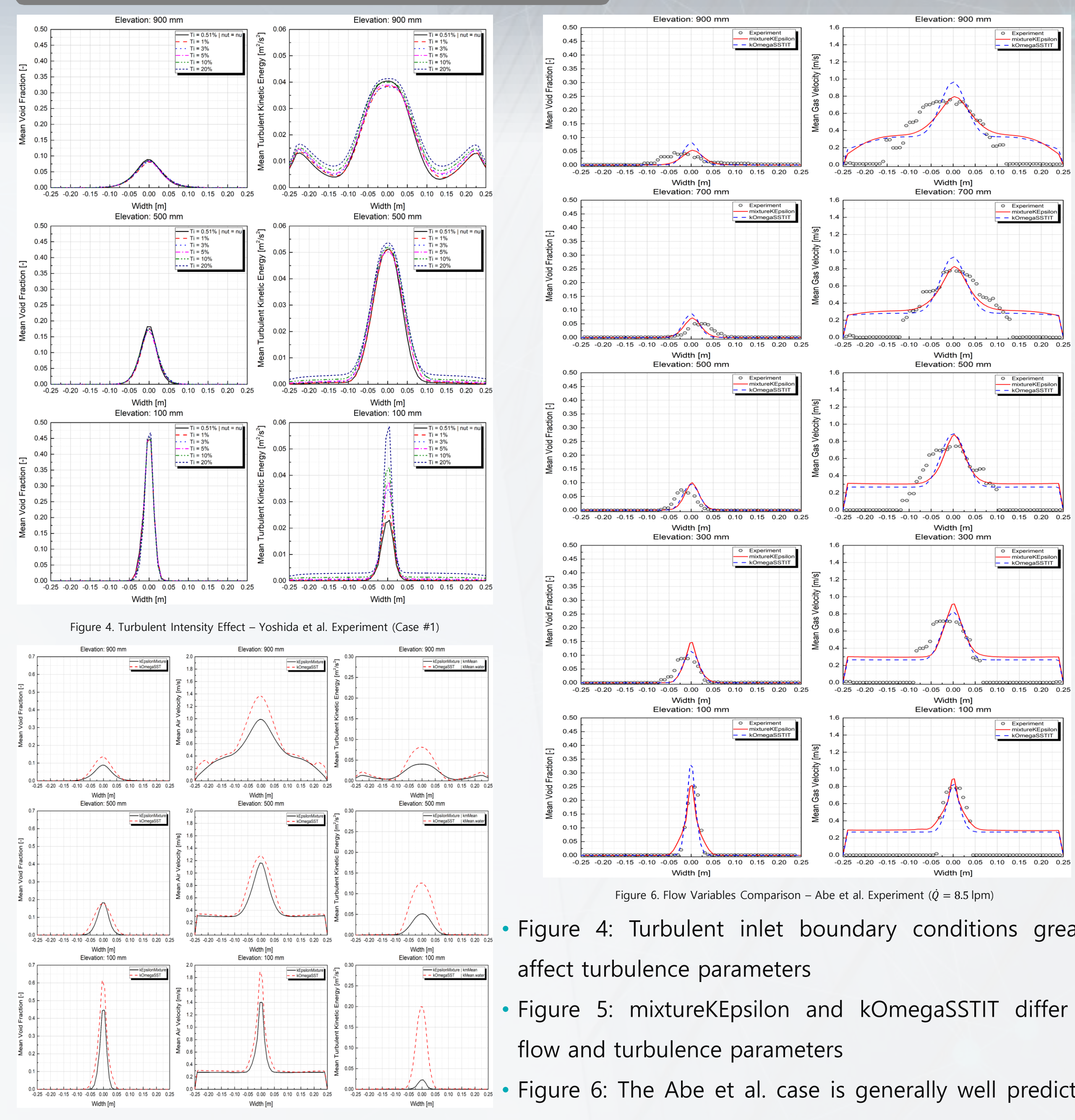


Figure 4. Turbulent Intensity Effect – Yoshida et al. Experiment (Case #1)

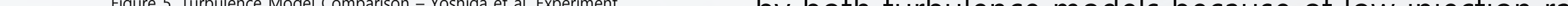


Figure 5: mixtureKEpsilon and kOmegaSST differ in flow and turbulence parameters

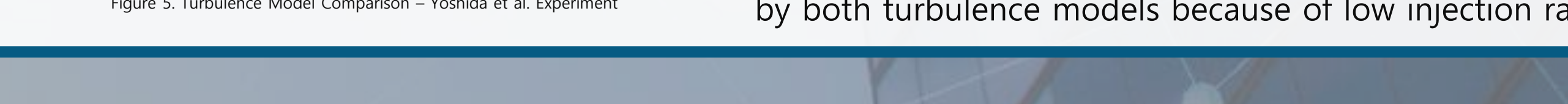


Figure 6: The Abe et al. case is generally well predicted by both turbulence models because of low injection rate

5. CONCLUSIONS

1 Inlet turbulent boundary conditions have a significant effect

- If the inlet Reynolds bubble number is in the laminar or transitional range, the inlet turbulent boundary conditions can be estimated by assuming $\nu_t \sim \nu_u$

- If the inlet Reynolds bubble number is in the turbulent range, the inlet boundary conditions can be estimated by assuming $\nu_t > \nu_u$; the resulting turbulent intensity is similar to that of pipe flow

2 Turbulence model has an effect on flow and turbulence parameters

- kOmegaSST predicts higher turbulent kinetic energy and lower turbulent viscosity than mixtureKEpsilon

3 Future Work

- The turbulent range of the inlet Reynolds bubble number necessitates further analysis
- The effect of turbulence model and boundary conditions on bubble size change should be investigated, e.g. by means of the Interfacial Area Transport Equation (IATE) or Population Balance Model (PBM)